Meteorol. Appl. 5, 000–000 (1998)

Modelling study of the IOP2 cold front of the FRONTS 87 experiment

Vassiliki Kotroni, Konstantinos Lagouvardos, George Kallos, *University of Athens, Meteorology Laboratory, Athens, Greece*
Yvon Lemaitre, *Centre pour l' Etude des Environnements Terrestre et Planetaire (CETP-CNRS), Velizy, France*

On 11–12 November 1987, a frontal system associated with an intense narrow cold frontal rainband was observed over the Channel between England and France. This case constitutes intensive observational period 2 (IOP2) of the FRONTS 87 experiment. It was an ideal example of upper-level and low-level jet coupling with substantial ascending motions and precipitation. The frontal system is analysed, in this paper, using the mesoscale non-hydrostatic model CSU/RAMS. The model uses a two-way interactive nested grid structure and full cloud microphysics parameterisation at various levels of complexity. The model results are compared with previous numerical investigations of this case as well as with observations obtained from the experimental network deployed during the campaign. The model succeeded in representing the frontal structure at meso- and convective scales, taking into account the large scale forcing; thus it is an important tool for the study of secondary cyclogenesis observed during the FASTEX campaign.

1. Introduction

FRONTS 87 was the first field observational campaign of the Mesoscale Frontal Dynamics Project (MFDP). This campaign lasted from 18 October 1987 until 13 January 1988 and was designed to provide an extended observational data set in order to study the structure, evolution and dynamics of cold fronts observed over the area centred on the Channel between England and France (Clough, 1987; Thorpe & Clough, 1991). Eight intensive observational periods (IOP) were defined during this campaign corresponding to the passage of eight cold fronts over the experimental site.

The IOP2 case study of FRONTS 87 has been the subject of several observational and modelling investigations in the past, owing to the interesting characteristics of the observed front. Doppler radar and dense sounding data analysis over Brittany (France) revealed that the front was characterised by strong line convection with intense vertical velocities (Chong *et al.*, 1991) while the frontal discontinuity was associated with a multiple low-level jet structure (Chong *et al.*, 1991; Kotroni & Lagouvardos, 1993). Thorpe & Clough (1991) analysed the thermodynamic structure of this front on the basis of drop-sounding data over the Atlantic Ocean south-west of the British Isles.

The interaction of the upper- and low-level jet-front system of IOP2 has been investigated with the aid of a mesoscale hydrostatic model (Sortais *et al.*, 1993). The authors provided a conceptual model showing the structure and orientation of the ageostrophic circulations associated with the upper- and low-level jets and analysed the dynamical and diabatic processes which contributed to the intensification of the low-level jet and the formation of the frontal band ahead of the cold front.

The dynamics of the rainbands and the line convection have been studied with the aid of a two-dimensional non-hydrostatic cloud model (Redelsperger & Lafore, 1994). The authors performed various sensitivity tests and concluded that with a 5 km horizontal grid, their model could provide a detailed and realistic simulation of the frontal system and the observed frontal bands. Moreover they investigated through analysis of the heat, moisture and horizontal momentum budgets the effects of the rainbands on larger scales.

The aim of the present paper is to provide further insight into the three-dimensional structure of the IOP2 cold front, with emphasis on the upper- and low-level jets as well as the narrow cold front rainband (NCFR), using a three-dimensional non-hydrostatic research model. This approach has the additional advantage that, for the detailed study of the IOP2 cold front, the three-dimensional synoptic-scale variations and interaction with other mesoscale features can be taken into account. The simulations have been performed using the Regional Atmospheric Modelling System (CSU-RAMS) developed at Colorado State University and the ASTER Division of the Mission Research Corporation. The nesting capabilities of this model provide an insight into the interaction of different scales and allow the NCFR to be resolved with a

horizontal resolution of 1.25 km. The results of the simulations will be compared with observations and the aforementioned modelling work. Moreover, this modelling exercise will permit the validation of RAMS capacity to represent the physical processes associated with frontal events, with the aim of using this model for the study of secondary cyclogenesis within the framework of the FASTEX experiment.

The description of the model as well as the model set-up are given in section 2. Section 3 is devoted to the presentation of the model results and the comparison of the simulated with the observed fields. The next three sections are devoted to a discussion of the results, and there are some concluding remarks in section 7.

2. Model and set-up

A detailed description of the RAMS model and its capacities is given in Pielke *et al.* (1992). However some of its features are summarised in the following:

- Two-way interactive nested grid structure (Clark & Farley, 1984).
- Terrain following coordinate surfaces with cartesian or polar stereographic horizontal coordinates.
- Cloud microphysics parameterisation at various levels of complexity (Tripoli & Cotton, 1980).
- Modified Kuo cumulus parameterisation (Tremback, 1990).
- Radiative transfer parameterisations (shortwave and longwave) through clear and cloudy atmospheres (Chen & Cotton, 1987).
- Various options for upper and lateral boundary conditions and for finite operators.
- Various levels of complexity for surface-layer parameterisation (soil-layer moisture and temperature model, vegetation parameterisation etc., McCumber & Pielke, 1981; Avissar & Mahrer, 1988).

For the present application, RAMS was initialised at 0000 UTC on 11 November 1987 and the duration of the simulation was 24 hours. The non-hydrostatic version of the model is employed, using four nested grids:

- Grid 1: with a mesh of 40 × 40 points and 60 km horizontal grid centred at 53° N and 5° W;
- Grid 2: with 74 × 89 points and 20 km horizontal grid, centred at the same point as the outer grid;
- Grid 3: with 98 × 110 points and 5 km horizontal grid, centred at 49.5° N and 3° W;
- Grid 4: with 125 × 125 points and 1.25 km horizontal grid, centred at 48.4° N and 4.5° W.

It should be noted that the fourth grid was activated only during the last 10 hours of simulation (from 1400 UTC on 11 November to 0000 UTC on 12 November), owing to the high CPU cost. The location and horizontal extension of each grid are presented in Figure 1.

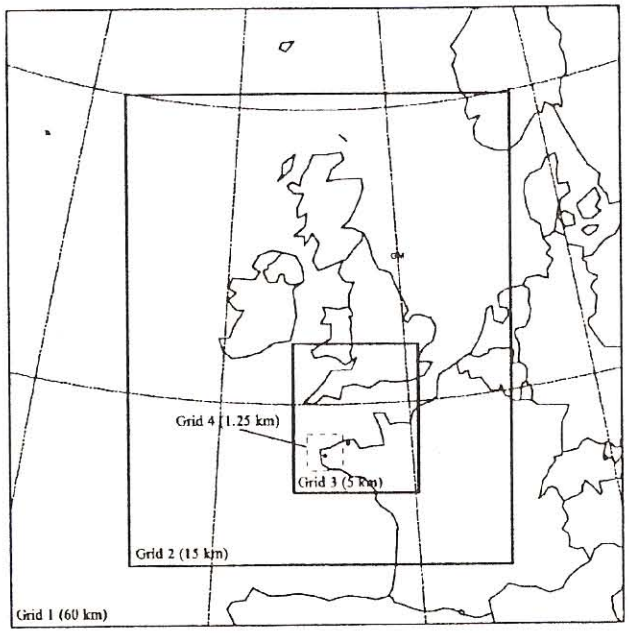

Figure 1. *Domain of the four nested grids of RAMS. For each grid the horizontal grid increment is given. The domain of the fourth nest is represented by a dashed-line rectangle while the star denotes the position of the C band Doppler radar near Brest (Brittany), which is referred to in the text. The open circle denotes the location of Lannion, the rawinsoundings release site.*

Twenty-seven levels following the topography were used on all grids. The vertical spacing varied from 120 m at the surface to 1 km at the top of the model (z = 16.5 km). Horizontal diffusion is based on the original Smagorinsky (1983) formulation, while vertical diffusion is parameterised according to the Mellor–Yamada (1974) scheme which employs a prognostic turbulent kinetic energy. Apart from these settings, a rigid lid was set at the top model boundary by constraining vertical velocity to be zero there. The lateral boundary conditions on the outer grid followed the Klemp–Lilly condition (Klemp & Lilly, 1978) with the vertical average of the gravity wave propagation speed at the boundaries. At the surface, a soil model developed by McCumber & Pielke (1981) and modified by Tremback & Kessler (1985) is used to predict the sensible and latent heat fluxes at the soil–atmosphere interface. Six soil levels were used down to 50 cm below the surface. Because one of the aims of the paper is to represent the microphysical structure of the observed front, the full microphysical package of RAMS is activated, which comprises condensation of water vapour to cloud water when supersaturation occurs as well as activation of microphysical parameterisation of rain, graupel, pristine ice, aggregates, and snow.

A modified Kuo-type cumulus parameterisation developed by Tremback (1990) is used because the model-resolved convergence produced at the scales of Grid 1 (60 km) and Grid 2 (20 km) is not enough to initiate convection explicitly. For Grid 3, the 5 km horizontal grid is too large a spacing to explicitly initiate convec-

tion but also too small to satisfy the assumptions in the cumulus parameterisation scheme. Cram *et al.* (1992) discussed the use of the cumulus parameterisation scheme in a simulation of a pre-frontal squall line. The authors found that the model encountered difficulties in explicitly triggering convection with a 5 km mesh, but they concluded that cumulus parameterisation should not be used on that scale. For that reason cumulus parameterisation was not activated for Grids 3 and 4.

The European Centre for Medium-Range Weather Forecasts (ECMWF) 1° latitude/longitude gridded analysis fields were used to initialise the model. The ECMWF data are objectively analysed by the RAMS model on isentropic surfaces from which they are interpolated to the RAMS grids. These fields were used in order to nudge the lateral boundary region of the coarser grid with a nudging time scale of 900 s. The influence of nudging extends five grid cells from the lateral boundary of the model domain (coarse grid). Climatological sea surface temperature of 1° horizontal resolution retrieved by the National Centre of Atmospheric Research (NCAR), topography derived from 30 s terrain data and gridded vegetation-type data of 10 min resolution have been used.

3. Observational evidence

At 1200 UTC on 11 November 1987, the IOP2 frontal system was associated with a 965 hPa low located north-west of Ireland (Figure 2), and reached the experimental area in Brittany during the late afternoon of 11 November 1987. Strong winds at the surface were reported by the synoptic network within the warm conveyor belt ahead of the cold front at 1800 UTC, with values exceeding 20 m s^{-1} over the south-western edge of England and Brittany. There were strong winds in general over the coastal areas of the Channel (Figure 3), while relatively weaker winds were observed over central France. At higher levels (850 hPa) the operational sounding network as well as the special soundings of FRONTS 87 reported south-westerly winds of 29–30 m s^{-1} over Brittany while over south-eastern England, Crawley upper-air station reported south-westerly winds of 32 m s^{-1} (not shown).

As the cold frontal system crossed the UK, it became apparent that it was characterised by complex features with more than one surface discontinuity. The first discontinuity was well marked and crossed Brittany at 2000 UTC, at 11 m s^{-1} from 315° (Chong *et al.*, 1991). At the surface a temperature drop of 2 °C and a surface wind veering by 25° were observed. The second discontinuity was less pronounced but the wind veered 20° further (Kotroni & Lagouvardos, 1993).

The two-dimensional frontal structure can be described by means of vertical cross-sections of the along-front wind component and the potential temperature field constructed from the rawinsoundings at Lannion. During all IOPs one sounding was performed about

Figure 2. *Surface map at 1200 UTC on 11 November 1987 with 5 hPa contour interval (from the European Meteorological Bulletin).*

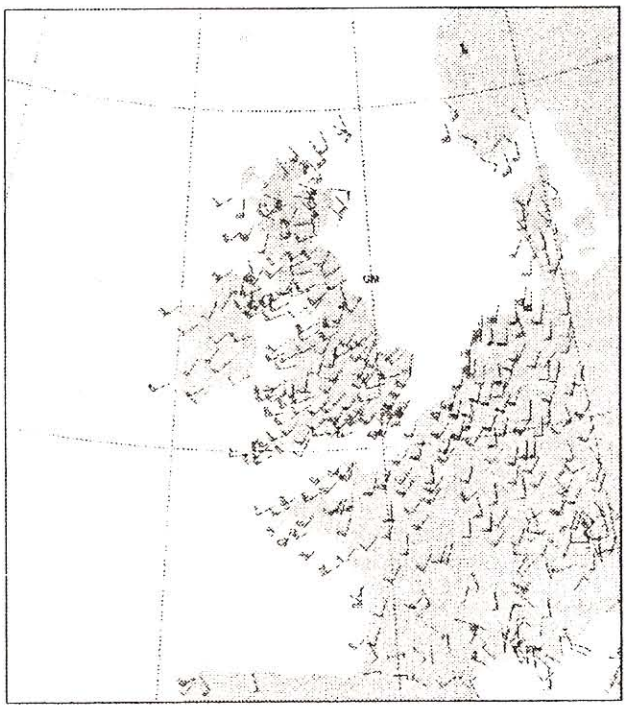

Figure 3. *Observed winds from the surface synoptic network at 1800 UTC on 11 November 1987. One pennant equals 20 m s^{-1}, one barb 4 m s^{-1} and one half-barb 2 m s^{-1}.*

every 60 min, with a vertical resolution of 30 m for the thermodynamic parameters and 120–150 m for the wind direction and intensity. More precisely during a period of 29 hours around the frontal passage over Lannion, at total of fourteen rawinsoundings were released. From the sounding analysis it was obvious that the frontal discontinuity was marked by a horizontal gradient of the potential temperature field at the lowest 2.5 km with a maximum of 3 K over 100 km (not shown). Moreover the front was associated with a strong cross-front gradient of the along-front wind component. Kotroni & Lagouvardos (1993) showed that the front was characterised by a multiple low-level jet (LLJ) structure, with two maxima of 34 m s^{-1} observed at z = 900 m and at z = 1100 m while a third maximum of 24 m s^{-1} was observed ahead of the second frontal discontinuity. A multiple LLJ structure has also been reported by Chong *et al.* (1991) on the basis of VAD analysis of Doppler radar observations near Brest with a maximum of 32.5 m s^{-1} at z = 1000 m just ahead of the frontal discontinuity. This LLJ structure is quite similar to a multiple LLJ front observed by Browning & Pardoe (1973). Analysis of the French operational forecasting system Peridot (with 35 km horizontal resolution) showed an LLJ with a maximum of 21 m s^{-1}

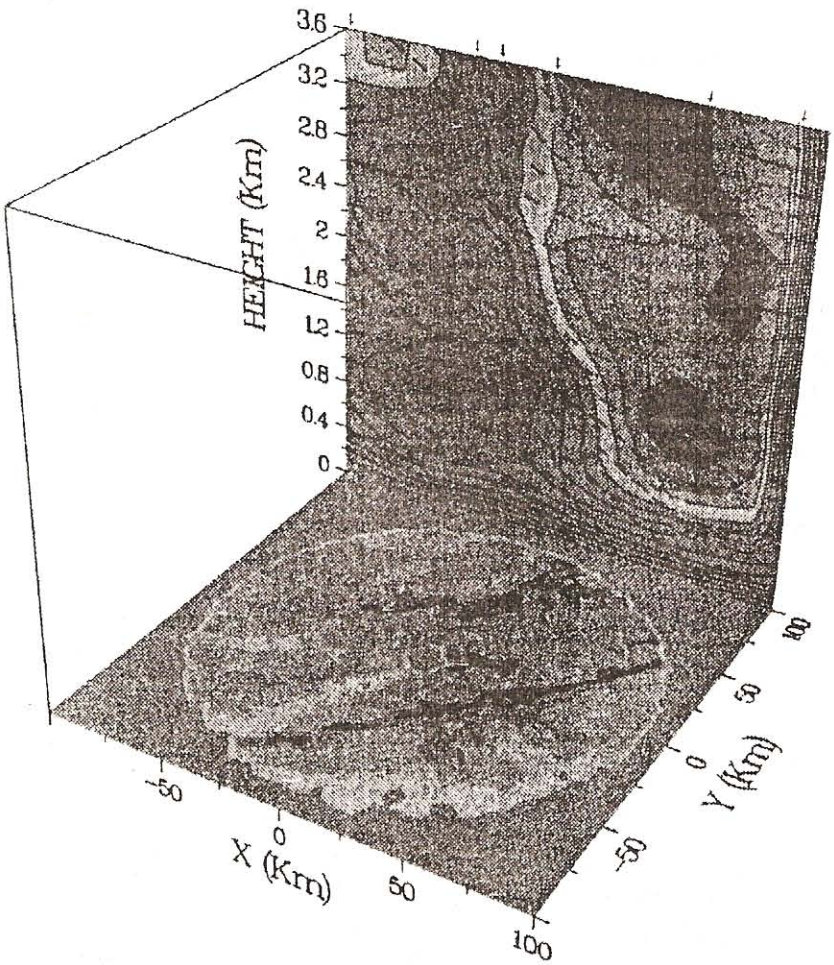

Figure 4. *Composite image consisting of a cross-section of the along-front wind component (coloured contours at 2 m s^{-1} interval) and potential temperature (dashed lines at 1 K interval) constructed from the soundings released from Lannion during IOP2 (small arrows indicate the time of sounding releases) and the reflectivity field (in dBZ) at 0.5 elevation from the PPI scan at 100 km range performed by the C band Doppler radar located near Brest.*

at the same height (Redelsperger & Lafore, 1994). This underestimation of the LLJ intensity has been attributed to the coarse model resolution.

A composite diagram consisting of a cross-section of the along-front wind component and of a reflectivity field is given in Figure 4. The cross-section has been constructed from the rawinsounding data set used by Kotroni & Lagouvardos (1993), and only a small domain extending vertically up to 3.6 km is presented. Six soundings have been used (separated in time by not more than 1.5 hours) which have been interpolated in time (at 30 min time intervals) using a cubic spline scheme. On the horizontal axis a time-to-space conversion has been performed and the domain shown corresponds approximately to a horizontal distance of 200 km. One of the two LLJ maxima of 34 m s^{-1} is evident at 1100 m. Note also the sharp decrease of the wind within the first 500 m, owing to surface friction. The reflectivity field from the PPI scan provided by the C band Doppler radar deployed near Brest is centred on the radar and covers a domain of 100 km × 100 km. A strong narrow cold frontal rainband (NCFR) appears as a narrow and enhanced reflectivity region with maximum values exceeding 30 dBZ. Distinct precipitation cores are evident within the NCFR, corresponding to distinct reflectivity maxima (exceeding 40 dBZ, dark red colour, in Figure 4). Chong *et al.* (1991), using a series of PPI scans performed by the same Doppler radar deployed near Brest, reported a mesoscale banded structure with embedded rainbands of 50 km width, 200 km in front of the frontal discontinuity and within the warm sector. The authors reported that the strong narrow cold frontal rainband, which was 5 km wide, was preceding a 50 km wide cold front rainband (WCFR). Moreover, radar observations from the UK network (Shutts, 1988) also reported a banded structure as well as a well-defined NCFR associated with the frontal system.

4. Low-level features

As already mentioned, the model was initialised at 0000 UTC on 11 November 1987. After 18 hours of model simulation, at 1800 UTC on 11 November, the RAMS model (Grid 1) predicted a low centre of 965 hPa north-west of Ireland (Figure 5). Some validation of the model results could be provided through comparison of the model predicted near-surface winds and the synoptic network reports given in Figure 3. RAMS predicted strong south-westerly winds of the order of 16 m s^{-1} with local maxima of 20 m s^{-1}, within the warm sector of the approaching cold front, over southern England, the Channel and offshore Brittany. The surface network also reported 16–20 m s^{-1} winds over the coastal areas of Britanny, Benelux and south-eastern England. Model-predicted winds over eastern England are slightly stronger than the reported winds. This could be partly attributed to the fact that the first

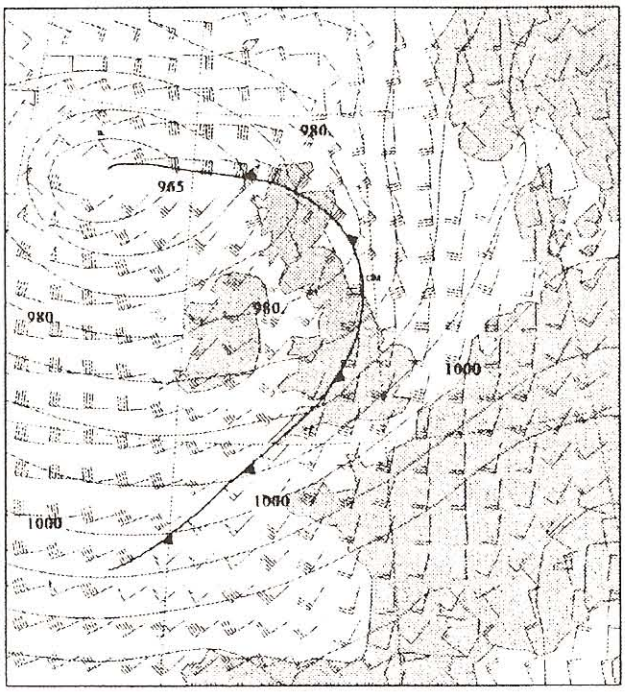

Figure 5. *Sea-level pressure (at 5 hPa interval) and winds at the first model level at 58 m AGL from Grid 1 of RAMS at 1800 UTC on 11 November 1987. One pennant equals 20 m s^{-1}, one barb 4 m s^{-1} and one half-barb 2 m s^{-1}.*

model level is at 58 m while the surface network reports winds at the anemometer level (12 m). At this point it should be noted that the model positions the frontal discontinuity about 40 km further west than its actual position. This can be attributed to the fact that the initialisation fields have a horizontal resolution of 1° latitude/longitude (80–90 km), which could have caused an uncertainty in the positioning of the front from the beginning of the simulation.

Figure 6(*a*) presents the equivalent potential temperature field, q_e, at z = 700 m AGL predicted by RAMS for Grid 2, at 2200 UTC on 11 November. This model level has been selected because sounding and model results showed that the most important horizontal gradients of the potential temperature and wind field at the low levels are confined in the layer 500–1200 m. The leading edge of the frontal discontinuity approximately coincides with the 304 K isopleth which extends from offshore Brittany through south-eastern England and to the east of Scotland. Inspection of the RAMS predicted potential temperature field revealed that the frontal discontinuity was marked by a potential temperature gradient of 3 K over a distance of 100 km in the area offshore Brittany (not shown). The area ahead of the frontal discontinuity and within the warm conveyor belt is characterised by high values of the along-front wind component (Figure 6(*b*)). The along-front wind component (estimated on the basis of the orientation of the frontal discontinuity from the 315° sector) exceeds 30 m s^{-1} over Brittany and the Channel and 35 m s^{-1} over south-eastern England. Note that at this level (700 m) the LLJ has more intense values over southern England than over Brittany, while surface

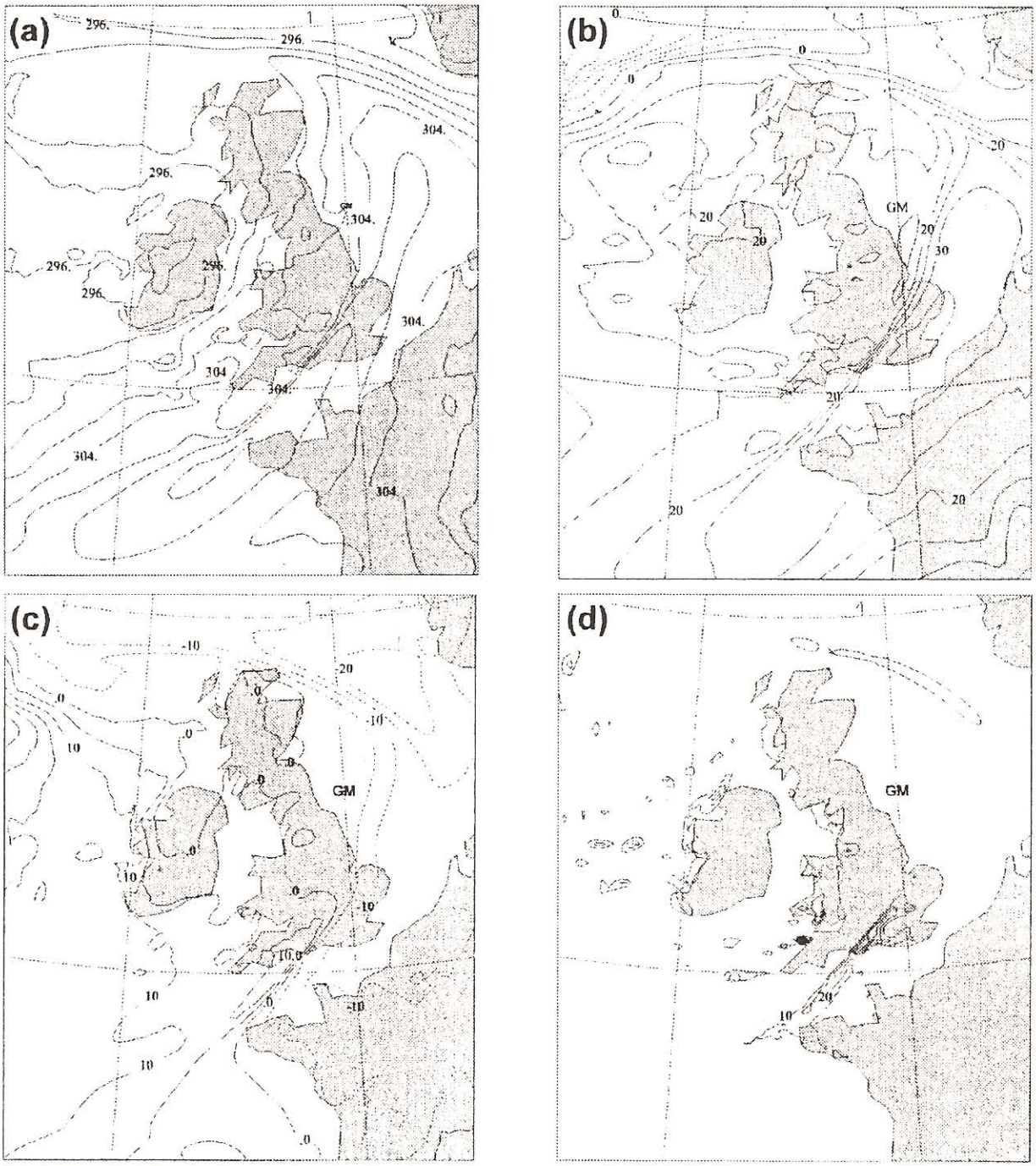

Figure 6. *(a) Horizontal cross-section of the equivalent potential temperature of Grid 2 of RAMS at 700 m AGL at 2200 UTC on 11 November 1987 (at 2 K interval). (b) As in (a), but for the along-front wind component (at 5 m s^{-1} interval). (c) Horizontal cross-section of the cross-front wind component, in the frame of reference moving with the front, from Grid 2 of RAMS at 190 m AGL (at 5 m s^{-1} interval). Negative values (dashed lines) denote inflow from the warm sector towards the cold front. (d) Horizontal cross-section of the vertical wind component from Grid 2 of RAMS at 700 m AGL (at 10 cm s^{-1} interval). Only values exceeding 10 cm s^{-1} are shown.*

winds, as reported by the synoptic network (Figure 3), are conversely more intense over Brittany than over southern England. This indicates that the LLJ does not have its maximum at the same level along the frontal discontinuity: in its northern part the maximum occurs at higher levels than in its southern part.

Figures 6(*a*) and 6(*b*) also reveal that the frontal discontinuity is characterised by an important transverse horizontal gradient of q_e and the along-front wind component. Following the successive position of the region of important transverse gradients during the elapsed 10 hours, the front has been estimated to propagate fairly steadily at a speed of the order of 10 m s^{-1}. This speed is consistent with the 11 m s^{-1} reported by the Doppler radars (Chong *et al.*, 1991).

On the cross-front wind field the convergence of warm air ahead and cold air behind the frontal discontinuity is more pronounced in the lower levels, especially

within the first 500 m. The cross-front wind component in the frame of reference moving with the front, at z = 190 m is given in Figure 6(*c*). The area from Brittany to southern England is characterised by important cross-front gradient. Note also the relative cross-front inflow, of the order of 5–10 m s^{-1}, at low levels going from the warm sector towards the NCFR. Chong *et al.* (1991) and Jaubert *et al.* (1991) identified this low-level cross-front inflow based on the analysis of the Doppler radar data over Brittany, reporting an inflow of the order of 10 m s^{-1} in the lowest 300 m.

The vertical wind component calculated by the model at z = 700 m AGL is given in Figure 6(*d*). A narrow band of ascent values exceeding 10 cm s^{-1} is depicted following the frontal discontinuity with a maximum of 48 cm s^{-1} over southern England. A second area of important updrafts is depicted in the cold sector, which might be associated with post-frontal activity.

5. Precipitation

The passage of the NCFR over Brittany was associated with heavy rain. The special surface network over Brittany recorded a maximum of 7 mm of accumulated precipitation within 1 hour associated with the frontal passage. The precipitation rate simulated by RAMS with Grid 3 is presented in Figure 7(*a*) (the precipitation rates are hourly averages). A band of heavy precipitation is evident over the Channel, oriented along the leading edge of the front, with the precipitation rate exceeding 10 mm h^{-1} over southern England (denoted by the letter B in Figure 7(a)). Over Brittany the precipitation rate is weaker, of the order of 3–4 mm h^{-1}, while over offshore northern Brittany the precipitation rate exceeds 7 mm h^{-1} (denoted by the letter A in Figure 7(*a*)). This precipitation pattern shows that at this resolution the model cannot explicitly resolve the NCFR intensity, at least over Brittany, where the dense surface raingauge network was deployed. Nevertheless, the spatial variability of precipitation within this NCFR is reproduced by Grid 3 with embedded cores of heavy precipitation (letters A, B). The existence of precipitation cores is common in mid-latitude fronts and several references can be found in the literature (James & Browning, 1979; Parsons & Hobbs, 1983; Hagen, 1992, among others). Inspection of successive fields of the total precipitation predicted by RAMS shows that the NCFR remains on the front while at the same time it drifts progressively along its length. The speed of motion of the NCFR along the length of the surface cold front has been estimated to be about 18 m s^{-1}. This drifting of the NCFR along the frontal discontinuity conforms with the observations reported by Hobbs & Biswas (1979), Hobbs & Persson (1982), Lemaitre & Brovelli (1990) and Kotroni *et al.* (1994).

With Grid 4 the convective precipitation can be explicitly resolved without use of a parameterisation scheme (Figure 7(*b*)). Redelsperger & Lafore (1994) suggested that 1 km resolution would be necessary in order to explicitly resolve the NCFR. In this study a 1.25 km resolution has been used in Grid 4. Distinct precipitation cores with total precipitation rates of the order of

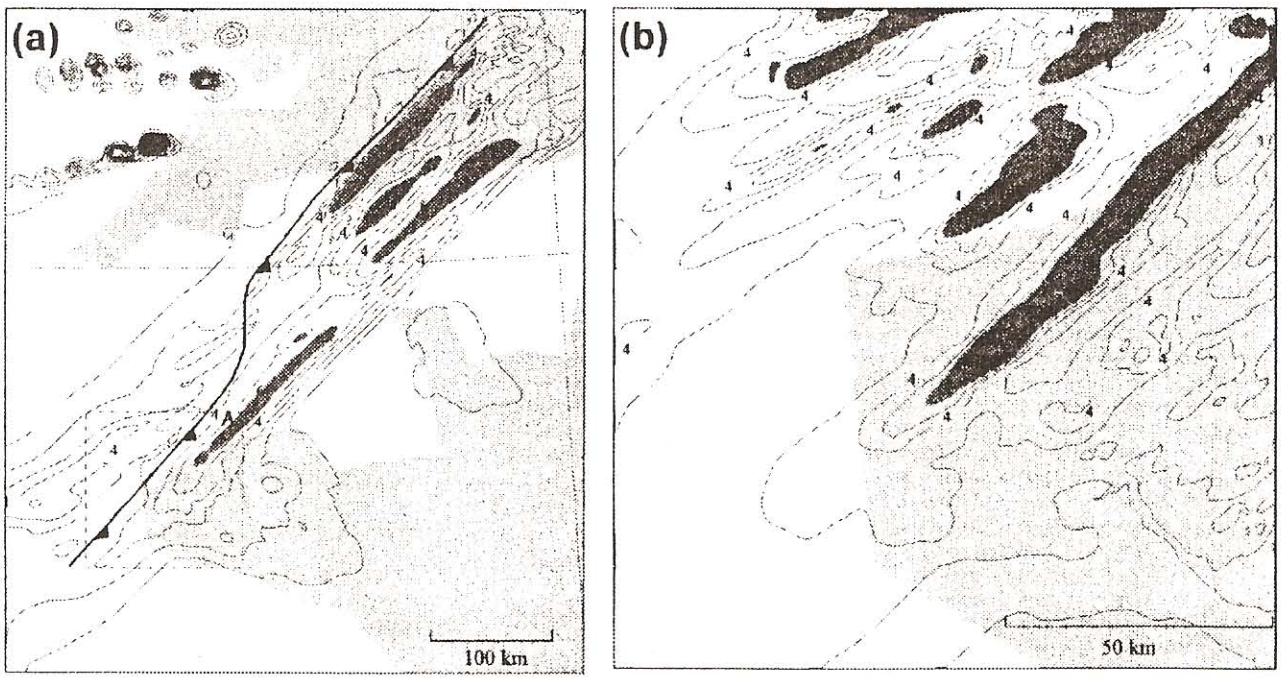

Figure 7. *(a) Total precipitation rate in Grid 3 of RAMS (at 1 mm h^{-1} interval) at 2200 UTC on 11 November 1987. The letters A and B denote the two precipitation cores discussed in the text. Dark shading denotes values greater than 6 mm h^{-1}. The dashed rectangle denotes Grid 4 shown in* (b) *and the cold front is shown with conventional symbols.* (b) *As in* (a) *but from Grid 4 of RAMS.*

14 mm h^{-1} are evident over Brittany. From the PPI reflectivity pattern given in Figure 4, a rough estimate of the precipitation rate based on the $Z = 200R^{1.6}$ relationship gives for 40–42 dBZ (which is the reflectivity maximum of the precipitation cores) a precipitation rate of 11–15 mm h^{-1}, which is in good agreement with the predicted one (if we take into account that Grid 4 and the PPI scan shown in Figure 4 have comparable horizontal resolutions). The updrafts associated with the NCFR activity are of the order of 2.5 m s^{-1} at a height of about 2.5 km (not shown); this is close to observations provided by dual Doppler techniques at 0.5 km horizontal resolution giving a 3 m s^{-1} vertical velocity within the NCFR updrafts (Chong *et al.*, 1991). Behind the NCFR the wide region of predicted precipitation is associated with the post-frontal activity. As observed by the ground stations and also reported by Chong *et al.* (1991) and Redelsperger & Lafore (1994), a wide cold frontal rainband (WCFR), 50 km in width, followed the NCFR.

6. Three-dimensional structure of the front

The three-dimensional structure of the cold front was investigated with the aid of the University of Wisconcin Vis-5D graphics package. The area investigated corresponds to Grid 2 of RAMS but bounded in altitude at 13 km. Figure 8(*a*) gives the three-dimensional structure of the 304 K isosurface of equivalent potential temperature. The selection of this parameter and the exact value of 304 K is based on inspection of the three-dimensional field of q_e; this can very well represent the three-dimensional structure of the frontal discontinuity. The warm sector is evident, characterised by q_e values greater than 304 K. On the same figure, a vertical cross-section of the along-front component is given. The upper-level jet is evident in the warm sector behind the surface cold front position. In addition, along with the q_e isosurface, the vertical velocity isosurface of 15 cm s^{-1} is plotted. Updrafts are evident along the frontal discontinuity at its leading edge from offshore Brittany through the Channel and southern England. This updraft region is located on the western side of the LLJ. Strong updrafts are confined within the first 2.5 km in altitude. This region of updrafts was also evident on the horizontal cross-section given in Figure 6(*d*).

Figure 8(*b*) gives a three-dimensional view of the relative position of the upper- and low-level jet at 2200 UTC. For this reason, the 45 m s^{-1} isosurface in the upper-tropospheric layers and the 28 m s^{-1} isosurface at the lower-tropospheric layers are plotted. The LLJ has a north-eastward orientation and it seems that its maximum occurs slightly higher at its northern than at its southern part. The indication of upward sliding of the LLJ maximum has been already mentioned from the comparison of the intensity of the LLJ over the Brittany and south-eastern England and the reports of the surface stations at the same locations. The relative position of the upper- and low-level jet conforms with the conceptual model proposed by Shapiro (1982) of a vertically coupled upper- and low-level jet. As can be inferred from Figure 8(*b*), the upper-level jet exit region is situated above the surface front and low-level jet. This coupling results in the enhancement of convection associated with the NCFR as the vertical branch of the upper-level indirect circulation links to the low level jet direct circulation associated with the cold front. Thus this coupling explains the intensity of the observed convection during this event. These results are also in good agreement with the findings of Sortais *et al.* (1993).

7. Conclusions

The frontal system of 11 January 1987 (IOP2) observed during the FRONTS 87 experiment has been studied with numerical simulations. The RAMS model has been used in order to perform non-hydrostatic three-dimensional simulations of the event, using four nested grids and full microphysics. The nesting capabilities of RAMS provided an insight into the three-dimensional structure of the system taking into account the interaction between the different scales of motion. Even with the coarser resolution of Grid 2 (20 km), the model was able to reproduce the frontal structure with the intense low-level jet, the temperature gradients marking the frontal discontinuity, the low-level cross-front inflow and the updrafts just ahead of the front. The full microphysics and the fine resolution of Grid 4 (1.25 km) allowed the NCFR, which was associated with the IOP2 cold front, to be explicitly resolved. The NCFR seemed to remain on the front while at the same time it also propagated at 18 m s^{-1} along the frontal discontinuity. Several precipitation cores have been identified within the NCFR. These not only conform with the radar observations for this case study but also with observational studies described in the literature. Moreover the three-dimensional representation of the wind field revealed the synergetic effects of the relative position of the upper- and low-level jets, leading to the intense convection observed during the passage of the front.

It should be noted that, though the model correctly reproduced the frontal progression speed, it positioned the frontal discontinuity about 40 km further west than its actual position during the whole simulation period. This can be attributed to the fact that the initialisation fields had a horizontal resolution of 1° latitude/longitude (80–90 km), which could have caused an uncertainty in the positioning of the front from the beginning of the simulation.

At this point one should note that simulations using four nested grids, the inner grid reaching a resolution of the order of 1 km, are extremely expensive in terms

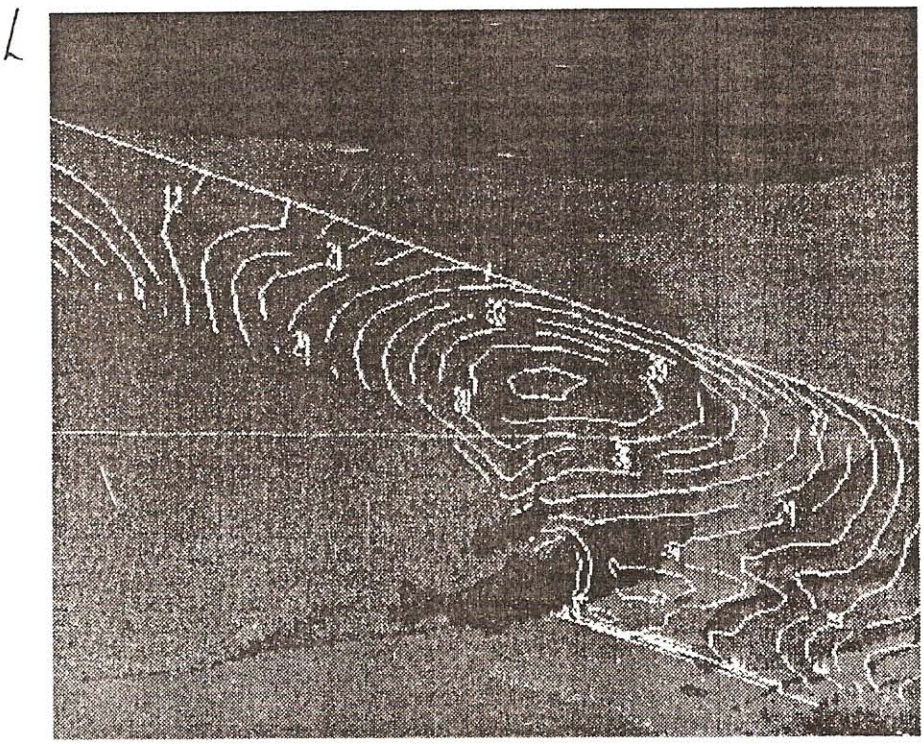

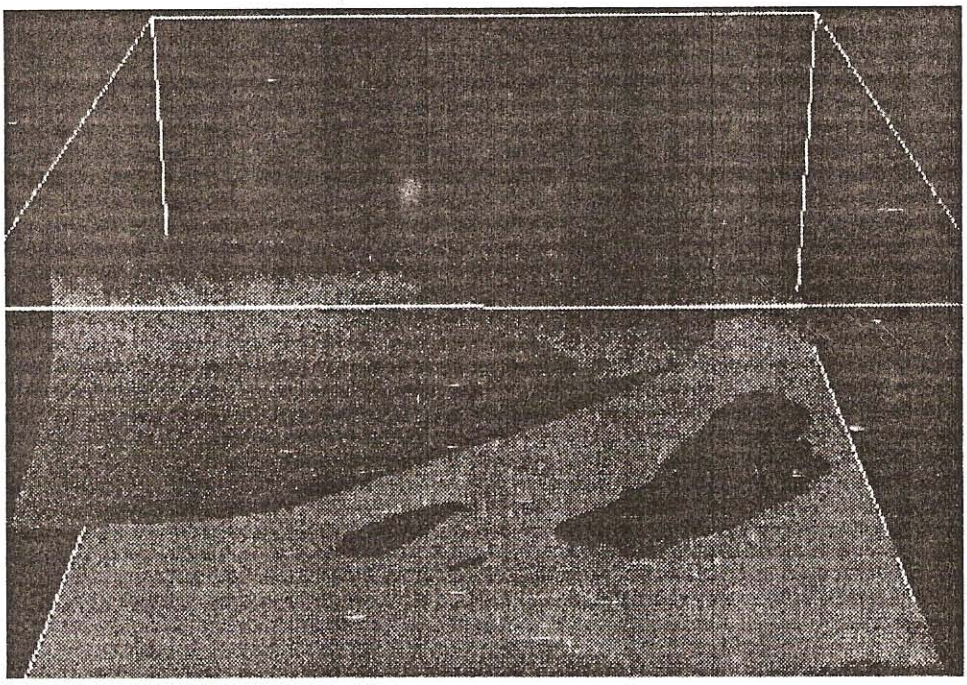

Figure 8. *(a) Three-dimensional structure of the cold front at 2200 UTC on 11 November 1987, within Grid 2 of RAMS but bounded in altitude at 13 km (constructed with the University of Wisconsin VIS-5D package). The 304 K equivalent potential temperature isosurface is represented by dark yellow, the 15 cm s^{-1} vertical velocity isosurface is represented by red while the along-front wind component is given at a cross-ection perpendicular to the front (at 3 m s^{-1} interval). (b) Three-dimensional structure of upper- and low-level jets. The 45 m s^{-1} isosurface (dark yellow) in the upper tropospheric layers and the 28 m s^{-1} isosurface (red) at the lower-tropospheric layers are plotted.*

of computer time (e.g. 1 hour of simulation was performed in 48 hours of wall-time). Very recently a parallel version of RAMS has become available and is being tested. This will facilitate the future use of the model in simulating such events as it will dramatically reduce the computer time consumption.

The RAMS model succeeded in representing the physical processes at meso- and convective scales for the IOP2 cold front. The promising results of this simulation make RAMS a useful tool for the study of the physics and dynamics of secondary cyclogenesis in the context of the FASTEX experiment.

Acknowledgements

This research has been partially supported by the Greek–French cooperative project PLATON (1996–1998). The authors are grateful to Dr C. Tremback (the ASTER Division of the Mission Research Corporation) for his helpful suggestions on the model settings and especially about the cumulus parameterisation scheme. Dr G. Scialom (CETP-IPSL) provided the necessary software for the radar imagery visualisation. Special thanks are also due to the editor, R. W. Riddaway, for his suggestions, which led to an improvement in the English and grammar of the text. The Centre National de Recherches Meteorologiques (CNRM–Météo France) provided the Lannion soundings as well as the data recorded by the special surface network in Britanny. Acknowledgement is also made to the National Center for Atmospheric Research, which is sponsored by the National Science Foundation, for some of the computing time used in this research and for providing the sounding and surface data from the operational network used in this study (Contract #35081147).

References

Avissar, R., & Mahrer Y., (1988). Mapping frost sensitive areas with a three dimensional local scale numerical model. Part I: Physical and numerical aspects. *J. Appl. Meteorol.*, **27**: 400–13.

Browning, K. A., & Pardoe C. W., (1973). Structure of low-level jet streams ahead of mid-latitude cold fronts. *Q. J. R. Meteorol. Soc.*, **99**: 619–38.

Chen, C., & Cotton, W. R., (1987). The physics of the marine stratocumulus-capped mixed layer. *Bound. Lay. Meteorol.*, **25**: 289–321.

Chong, M., Jaubert G., & Nuret M., (1991). Small scale structure of a cold-frontal rainband. In *Preprints 25th International Conference on Radar Meteorology*, Am. Meteorol. Soc., Boston, 181–4.

Clark, T. L. & Farley, R. D. (1984). Severe downslope windstorm calculations in two and three spatial dimensions using anelastic interactive grid nesting: a possible mechanism for gustiness. *J. Atmos. Sci.*, **41**: 329–50.

Clough, S. A. (1987). The mesoscale frontal dynamics project. *Meteorol. Mag.*, **116**: 32–42.

Cram, J. M., Pielke, R. A. & Cotton, W. R. (1992). Numerical simulation and analysis of a prefrontal squall line. Part II: Propagation of the squall line as an internal gravity wave. *J. Atmos. Sci.*, **49**: 209–25.

James, P. K & Browning, K. A. (1979). Mesoscale structure of line convection at surface cold fronts. *Q. J. R. Meteorol. Soc.*, **105**: 371–82.

Jaubert, G., Nuret, M. & Chong, M. (1991). A case study of cold-frontal rainbands. In *Preprints of 25th International Conference on Radar Meteorology*, Am. Meteorol. Soc., Boston, 185–8.

Hagen, M. (1992). On the appearance of a cold front with a narrow rainband on the vicinity of the Alps. *Meteorol. Atmos. Phys.*, **48**: 231–48.

Hobbs, P. V. & Biswas, K. R. (1979). The cellular structure of narrow cold-frontal rainbands. *Q. J. R. Meteorol. Soc.*, **105**: 723–7.

Hobbs, P. V. & Persson, O. G. (1982). The mesoscale and microscale structure and organisation of clouds and precipitation in midlatitude cyclones. Part V: The substructure of narrow cold-frontal rainbands. *J. Atmos. Sci.*, **39**: 280–95.

Klemp, J. B. & Lilly, D. K. (1978). Numerical simulation of hydrostatic mountain waves. *J. Atmos. Sci.*, **35**: 1070–96.

Kotroni, V. & Lagouvardos, K. (1993). Low-level jet streams associated with atmospheric cold fronts: seven case studies from the FRONTS 87 experiment. *Geophys. Res. Lett.*, **20**: 13, 1371–4.

Kotroni, V., Lemaitre, Y. & Petitdidier, M. (1994). Dynamics of a low-level jet observed during the FRONTS 87 experiment. *Q. J. R. Meteorol. Soc.*, **120**: 277–303.

Lemaitre, Y. & Brovelli, P. (1990). Role of a low level jet in triggering and organising moist convection in a baroclinic atmosphere. A Case study: 18 May 1984. *J. Atmos. Sci.*, **47**: 82–99.

McCumber, M. C. & Pielke, R. A. (1981). Simulation of the effects of surface fluxes of heat and moisture in a mesoscale numerical model. Part I: Soil layer. *J. Geophys. Res.*, **86**: 9929–38.

Mellor, G. L. & Yamada, T. (1974). A hierarchy of turbulence closure models for planetary boundary layers. *J. Atmos. Sci.*, **31**: 1791–1806.

Parsons, D. B. & Hobbs, P. V. (1983). The mesoscale and microscale structure and organization of clouds and precipitation in midlatitude cyclones. Part XI: Comparison between observational and theoretical aspects of rainbands. *J. Atmos. Sci.*, **40**: 2377–97.

Pielke, R. A, Cotton, W. R., Walko, R. L, Tremback, C. J., Lyons, W. A, Grasso, L. D., Nicholls, M. E., Moran, M. D., Wesley, D. A., Lee, T. J. & Copeland, J. H. (1992). A comprehensive meteorological modelling system – RAMS. *Meteorol. Atmos. Phys.*, **49**: 69–91.

Redelsperger, J.-L., & Lafore, J-P (1994). Non-hydrostatic simulations of a cold front observed during the FRONTS 87 experiment. *Q. J. R. Meteorol. Soc.*, **120**: 519–56.

Shapiro, M. (1982). *Mesoscale weather systems of the central United States.* Cooperative Institute of Research in Environmental Sciences, University of Colorado/NOAA, Boulder, 78 pp.

Shutts, G. J. (1988). Mesoscale Frontal Dynamics Project FRONTS 87, Quicklook Atlas. *Report No. 6, University of Reading.*

Smagorinsky, J. (1963). General circulation experiments with the primitive equations. Part I. The basic experiment. *Mon. Wea. Rev.*, **91**: 99–164.

Sortais, J.-L., Cammas, J.-P., Yu, X. D., Richard, E. & Rosset, R. (1993). A case study of coupling between low- and upper-level jet-front systems: investigation of dynamical and diabatic processes. *Mon. Wea. Rev.*, **121**: 2239–53.

Thorpe, A. J. & Clough, S. A. (1991). Mesoscale dynamics of cold fronts. I: Structures described by dropsoundings in FRONTS 87. *Q. J. R. Meteorol. Soc.*, **117**: 903–41.

Tremback, C. J. (1990). Numerical simulation of a mesoscale convective complex: model development and numerical results. Ph.D. dissertation, *Atmos. Sci. Paper No. 465, Colorado State University, Dept. of Atmos. Science*, Fort Collins, Co 8523.

Tremback, C. J. & Kessler, R. (1985). A surface temperature

and moisture parameterisation for use in mesoscale numerical models. In *Preprints, 7th AMS Conference on Numerical Weather Prediction*, 17–20 June, Montreal, Canada, Am. Meteorol. Soc., Boston, 355–8.

Tripoli, G. J. & Cotton, W. R. (1980). A numerical investigation of several factors contributing to the observed variable intensity of deep convection over south Florida. *J. Appl. Meteorol.*, **19**: 1037–63.